LA-UR- 11-01064

Approved for public release; distribution is unlimited.

Title:	Ultrafast density-and-temperature-dependent carrier dynamics in a quantum dots-in-a-well heterostructure
Author(s):	R. P. Prasankumar, R. V. Shenoi, J. Urayama, W. W. Chow, S. Krishna, and A. J. Taylor
Intended for:	SPIE Photonics West, San Francisco, CA, USA

Form 836 (7/06)

Ultrafast density-and-temperature-dependent carrier dynamics in a quantum dots-in-a-well heterostructure

R. P. Prasankumar*[a], R. V. Shenoi[b], J. Urayama[c], W. W. Chow[c], S. Krishna[b], and A. J. Taylor[a]
[a]Center for Integrated Nanotechnologies, Los Alamos National Laboratory, Los Alamos, NM 87545;
[b]Department of Electrical and Computer Engineering, Center for High Technology Materials, University of New Mexico, Albuquerque, NM 87106
[c]Sandia National Laboratories, Albuquerque, NM 87123

ABSTRACT

The incorporation of semiconductor quantum dots into different heterostructures for applications in nanoscale photodetection, lasing and amplification has been an active area of research in recent years. Here, we use ultrafast differential transmission spectroscopy to temporally and spectrally resolve density-and-temperature-dependent carrier dynamics in an InAs/InGaAs quantum dots-in-a-well (DWELL) heterostructure. In our experiments, electron-hole pairs are optically injected into the three dimensional GaAs barriers, after which we monitor carrier relaxation into the two dimensional InGaAs quantum wells and the zero dimensional InAs quantum dots by tuning the probe photon energy. We find that for low photoinjected carrier densities, carrier capture and relaxation are dominated by Auger carrier-carrier scattering at low temperatures, with thermal emission playing an increasing role with temperature. At low temperatures we also observe excitation-dependent shifts of the quantum dot energy levels. In contrast, high density measurements reveal an anomalous induced absorption at the quantum dot excited state that is correlated with quantum well population dynamics. Our experiments provide essential insight into carrier relaxation across multiple spatial dimensions and reveal unique Coulomb interaction-induced phenomena, with important implications for DWELL-based lasers and amplifiers.

Keywords: Ultrafast dynamics, quantum dots, dots-in-a-well, ultrafast phenomena, semiconductor heterostructures

1. INTRODUCTION *

Low dimensional semiconductor nanostructures have attracted much attention due to the unique size-dependent scaling of their physical properties, providing researchers an opportunity to tune these parameters in a manner not afforded by naturally occurring bulk materials. The intriguing physics in these systems, along with their immense potential for applications in areas including electronics and photonics, has driven an intense research effort aimed at understanding and controlling their properties. The most heavily studied nanostructures are two-dimensional (2D) quantum wells (QWs) and zero-dimensional (0D) quantum dots (QDs), since high quality samples can be readily fabricated, most often through epitaxial self-assembly or colloidal chemistry.[1, 2] The unique optical characteristics of these nanosystems make them ideal for photonic applications including infrared photodetection[3] and semiconductor lasing.[4] However, in order to optimize device properties such as power consumption and modulation speed, a comprehensive understanding of non-equilibrium density-and-temperature-dependent carrier dynamics in these nanostructures is vital. Therefore, an extensive body of research has focused on a detailed characterization of carrier dynamics in QWs and QDs after pulsed optical excitation.[5, 6] Despite the intense effort in this area, very few time-resolved optical studies have been performed on heterostructures intentionally designed to display multiple degrees of spatial confinement. This is an important avenue of study, as combinations of two-dimensional, one-dimensional, and zero-dimensional nanostructures are beginning to find many photonic applications.

A well-known example of this concept is the dots-in-a-well (DWELL) heterostructure, which combines quantum wells and quantum dots in an effort to overcome the limitations of conventional QW-and-QD-based photodetectors and lasers.[7] These restrictions include the inability of conventional quantum well infrared photodetectors (QWIPs) to

*rpprasan@lanl.gov; phone 1 505 284-7966; fax 1 505 284-7778; http://cint.lanl.gov

operate at normal incidence without the fabrication of gratings and other structures to couple light into the device. Quantum-dot infrared photodetectors (QDIP) have also been used in a variety of settings, but are limited by thermal emission and difficulties in control of the operating wavelength. In addition, QW-and-QD-based lasers suffer from relatively high thresholds and low gain.[4]

The DWELL design offers an appealing approach towards overcoming these limitations. These heterostructures, typically grown by molecular beam epitaxy (MBE), are based on InAs quantum dots placed in a thin InGaAs quantum well (QW) that is subsequently sandwiched between GaAs barrier layers.[3, 7] This lowers the ground state of the QD relative to the GaAs band edge, reducing thermal emission in DWELL-based photodetectors. In addition, by altering the thickness and composition of the InGaAs well surrounding the dots, the position of the excited state can be varied without changing the QD ground state, enabling control of the operating wavelength in a DWELL photodetector. Confinement of electrically injected carriers to a two dimensional QW also increases the QD density and efficiency of carrier capture by the QDs. This has led to record low threshold currents, improved temperature stability, and higher modal gain in DWELL-based lasers.[4, 8]

However, further advances in DWELL technology will require ultrafast spectroscopic techniques to improve understanding of carrier relaxation and transport in these novel nanostructures. For example, despite the many impressive achievements of DWELL-based lasers, their limited modulation bandwidth has restricted their use in certain applications.[1, 9-11] This is primarily because carrier relaxation through discrete QD levels after injection into the barriers is generally slower than in bulk and QW systems, although electron-hole scattering and tunneling injection have been shown to increase relaxation rates.[1, 11] In addition, Coulomb carrier-carrier interactions strongly influence dynamics at the high densities relevant to laser operation by modifying relaxation rates and introducing time-dependent energy level shifts.[11-16] An understanding of high-density carrier dynamics is therefore critical for further advances in QD laser and amplifier technology.

In this work, we perform temperature and wavelength dependent differential transmission (DT) spectroscopy to examine carrier relaxation in a DWELL heterostructure. Although some time-resolved measurements have been performed on quantum dots-in-a-well structures,[17-22] few have aimed at understanding the influence of multiple degrees of spatial confinement on carrier dynamics. Our pump-probe measurements of carrier relaxation in a DWELL heterostructure after photoexcitation of electron-hole pairs in the barriers allow us to temporally resolve carrier relaxation across multiple spatial dimensions, from the three dimensional (3D) barriers into 2D quantum well and 0D quantum dot states, by simply tuning the probe wavelength.

Our experiments demonstrate that carrier dynamics in the DWELL system at low densities is dominated by Auger-type carrier-carrier scattering, with electron-electron scattering governing electron capture from the QW into the QD excited state and electron-hole scattering efficiently relaxing electrons from the QD excited state to the QD ground state.[23] At higher temperatures, we find that thermal emission plays a significant role, causing carriers to be distributed over many adjacent levels in the DWELL heterostructure. Furthermore, density-dependent experiments at low temperatures reveal Coulomb interaction-induced shifts of the QD energy levels at low carrier densities, while at high carrier densities we observe a strong influence of the QW population upon light absorption at the QD excited state.[24] This unique phenomenon has not previously been observed in DWELL heterostructures and will significantly impact the operation of DWELL-based lasers and amplifiers. Overall, our experiments provide fundamental insight into carrier relaxation in a system designed to exhibit multidimensional quantum confinement, along with information relevant to optimizing performance in DWELL-based photodetectors and lasers.

2. SAMPLE FABRICATION AND EXPERIMENTAL SETUP

2.1 Sample fabrication

The DWELL device structure is depicted in Figure 1(a). It is composed of 15 layers, each consisting of 2.4 ML of InAs QDs (density~4.6×10^{10} cm^{-2}) grown on a 1 nm InGaAs QW, capped by a 6 nm InGaAs QW, and placed in a GaAs matrix; further growth details are described in references [3] and [25]. The QDs are doped with ~1 electron/dot for detector applications. The semi-insulating GaAs substrate was etched off in a ~5x5 mm^2 region to eliminate any influence on the measured signals.

Intensity-dependent photoluminescence (PL) experiments[13, 26] were performed to characterize the interband optical transitions in the DWELL heterostructure. Figure 1(b) depicts PL measurements taken on our DWELL sample at 77 K.

Gaussian curve fits to the 77 K data reveal two QD interband transitions, with the QD excited (n=2) state centered at 1050 nm (1.18 eV) and the ground (n=1) state centered at 1109 nm (1.12 eV). The width of these peaks is due to inhomogeneous broadening of the dot size distribution. The QW n=2 and n=1 states are centered at 880 nm (1.41 eV) and 935 nm (1.33 eV), respectively. These interband transitions in the QDs and QWs are due to electron and hole levels with the same quantum number n. After increasing the temperature to 295 K (Fig. 1(c)), the PL peaks shift to longer wavelengths, as expected from the temperature dependence of the bulk GaAs and InAs band gaps. The center wavelengths are 1115 nm (1.12 eV) and 1192 nm (1.04 eV) for the n=2 and n=1 transitions, respectively. The center wavelengths of the two lowest QW interband transitions are 912 nm (1.36 eV) and 1001 nm (1.24 eV). This allowed us to draw schematics of the DWELL energy levels at low temperatures (Fig. 1(d)), assuming a 60:40 energy splitting between conduction and valence bands. The energy levels depicted in Fig. 1(d) are average values, as individual dots within the inhomogeneously broadened size distribution may have a different energy level structure.

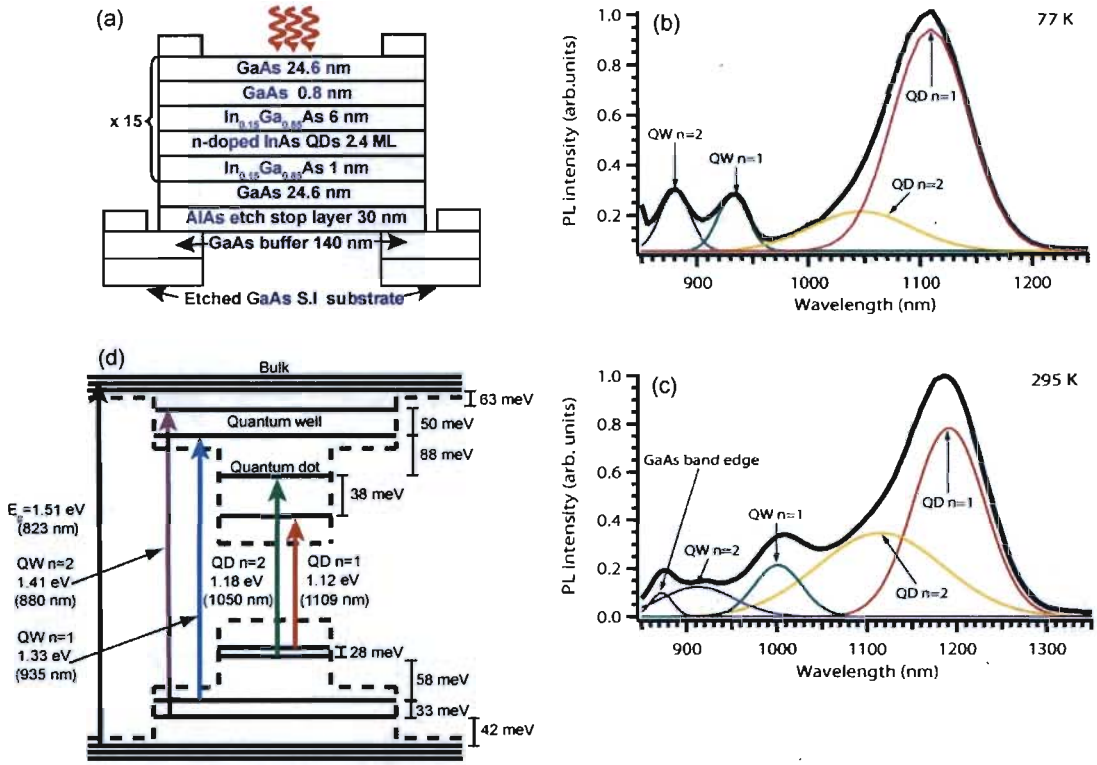

Figure 1. (a) Schematic of the DWELL structure. (b) PL spectrum at 77 K. (c) PL spectrum at 295 K. (d) Low temperature energy level schematic. Reprinted from ref. [23] with permission.

2.2 Experimental setup

Optical pump-probe experiments were based on a 100 kHz regeneratively amplified Ti:sapphire laser system producing 50 fs, 10 μJ pulses at 800 nm. The output beam is split into two equal parts to concurrently pump two optical parametric amplifiers (OPA). The visible OPA produces a signal beam tunable from 480-700 nm, an idler beam tunable from 930-2300 nm, and a residual pump beam at 400 nm. Similarly, the IR OPA produces a signal tunable from 1.1-1.6 μm and an idler tunable from 1.6-3.3 μm, with a residual pump at 800 nm. This enables measurements with independently tunable pump and probe wavelengths over a range of 400 nm (3.1 eV) to 3.3 μm (0.38 eV) and sub-100 fs time resolution (Figure 2).

Temperature-dependent differential transmission (DT) measurements were performed near normal incidence with a pump wavelength of 800 nm (1.55 eV) and fluences ranging from 2.8-28 μJ/cm^2. This excites a carrier density of $1.8\text{x}10^{11}$-$1.8\text{x}10^{12}$ cm^{-2} in the GaAs barrier layers, corresponding to a density range of 4 to 40 electron-hole pairs (ehp) per dot. The probe wavelength was tuned from 939-1250 nm (0.99-1.32 eV) at each temperature to track carrier relaxation in the DWELL heterostructure. This range of probe wavelengths allowed us to examine carrier capture and

relaxation processes in the lowest QW (n=1) state and both QD states at low temperatures; at high temperatures the low energy side of the QW n=2 state also overlaps with the high energy side of our probe spectrum. It is worth noting that due to the relatively large size distribution of our QDs and broad bandwidth (~30 nm) of our probe pulses, the DT signal at certain probe wavelengths (particularly 1074 and 1103 nm) includes contributions from both QD n=1 and n=2 states. Therefore, when analyzing time dependent traces, we only consider probe wavelengths at which the contribution of the transition of interest to the DT signal is at least a factor of 5 greater than that of any other transition, as estimated from the measured PL spectra.

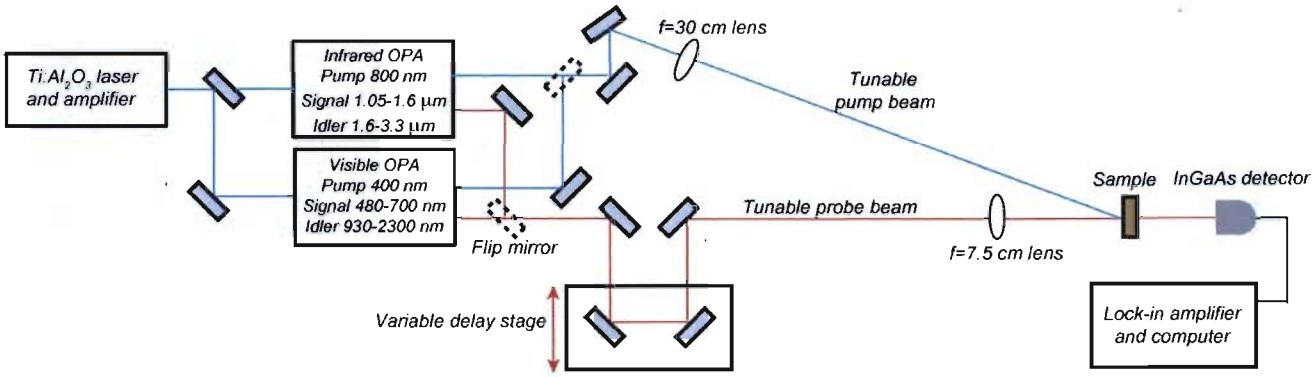

Figure 2. Experimental setup for ultrafast wavelength-tunable optical spectroscopy.

3. ULTRAFAST CARRIER DYNAMICS AT LOW TEMPERATURES AND LOW CARRIER DENSITIES

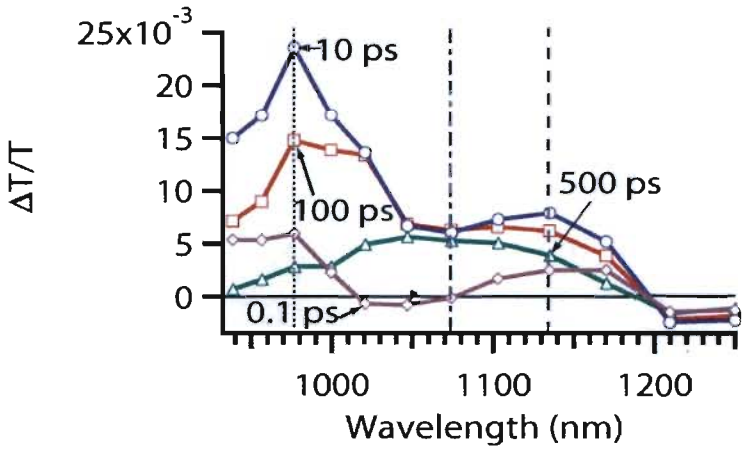

Figure 3. Differential transmission spectrum taken at 30 K at N=4 ehp/dot. The approximate positions of the QW n=1, QD n=2, and QD n=1 states are indicated by the dotted, dot-dashed, and dashed lines, respectively. Reprinted from ref. [23] with permission.

Figure 3 depicts the differential transmission spectrum at an excitation level of N=4 ehp/dot for time delays of t=0.1, 10, 100, and 500 ps at 30 K. The DT signal is proportional to the sum of the electron and hole occupations of the QD levels;[26, 27] therefore, our DT measurements can directly track the temporal evolution of carrier populations in the DWELL heterostructure. The peak positions indicated in the 30 K DT spectrum of Fig. 3 are red shifted from those obtained through PL measurements (Fig. 1(b)), likely due to the significantly lower carrier density used in the DT experiments[12, 26, 28] The DT signal at t=0.1 ps clearly shows that optically excited carriers rapidly populate the QW and QD n=1 states. However, this signal is negative for a band of wavelengths around the QD n=2 state (1021-1074 nm). Density-dependent measurements (section 5) indicate that this negative signal increases in amplitude and persists for longer times with increasing excitation density. There is also a negative DT signal for long wavelengths (1200-1250 nm) which remains at long time delays, quite similar to that observed in ref. [26]. These negative signals will be

discussed in much more detail below in section 5; in this section, we will focus on low temperature dynamics at N=4 ehp/dot, at which the energy level schematic depicted in Fig. 1(d) can reliably be used to interpret our data.

The "camel back" shaped DT spectrum reveals that all energy levels within the heterostructure are maximally populated by t=10 ps. From Fig. 3, it can be seen that the carriers leave the QW states on a time scale of a few hundred ps and are captured into the QDs, fully depopulating the QWs in ~500 ps. A particularly long relaxation is observed at the QD n=2 state, where curve fits indicate that the DT signal decays with a ~2.5 ns time constant. The DT signal at the ground state decays more rapidly, with a time constant of ~1 ns. More insight into carrier dynamics in the DWELL heterostructure can be obtained by examining the time dependence of the DT signal at different probe energies.

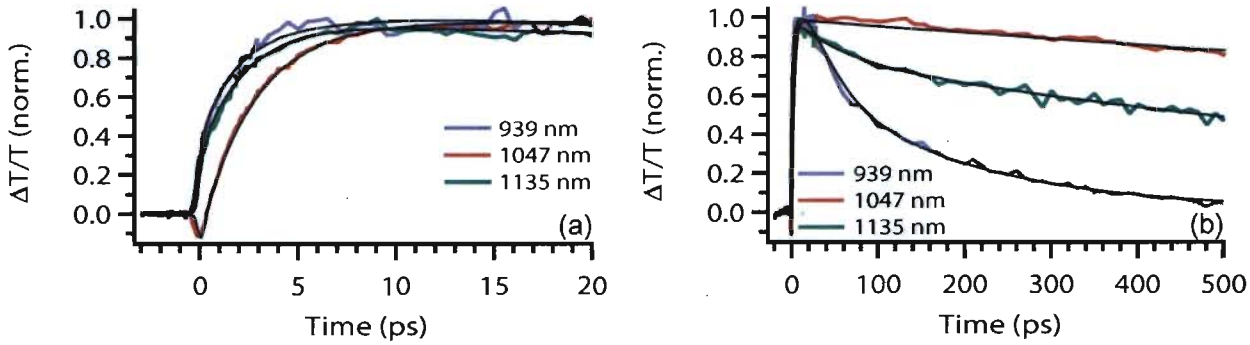

Figure 4. Normalized 30 K time-dependent DT signals for N=4 ehp/dot at the QW n=1 (977 nm) state, QD n=2 (1047 nm) and QD n=1 (1135 nm) states at (a) short and (b) long time delays. Reprinted from ref. [23] with permission.

Figure 4 depicts low temperature time-dependent DT traces at the QW n=1, QD n=2, and QD n=1 states at early (a) and late (b) times. By analyzing this data, we can discern the relative contributions of processes including relaxation through a finite continuum of states, carrier-phonon scattering, electron-electron scattering, and electron-hole scattering to carrier capture and relaxation within the DWELL heterostructure. We first compare the time-resolved DT traces at early times (Fig. 4(a)) to understand carrier capture dynamics. The rise times of these signals (~2-4 ps), due to carrier capture into QW and QD states, are comparable across the measured wavelength range, indicating that carriers are relaxing into the QD states at rates comparable with the relaxation into the lowest QW state. This contrasts with previous DT measurements on self-assembled InAs QDs at low excitation densities of <1 ehp/dot, in which a sequential relaxation of electrons from the n=2 to the n=1 state was observed.[13, 29] Our results do compare well with time-resolved PL measurements on a similar DWELL structure, in which the rise times of the PL signal from the QW and both QD states were ~6 ps.[19] This was attributed to carrier relaxation through a finite continuum of states, allowing carriers to rapidly populate QD states through phonon emission.[30] However, this is likely not the operative mechanism for QD carrier capture in our measurements, as will be demonstrated below.

Carrier capture into the QWs and QDs can instead be understood as follows: after photoexcitation in the GaAs barriers, electrons and holes are captured by the QW and quickly relax to the lowest QW state through phonon emission,[5] bleaching it within ~2 ps as seen in Fig. 4(a). The holes will simultaneously relax through the densely spaced valence band levels through LO and LA phonon emission, populating the lowest QD states on a sub-ps time scale.[26] This causes the initial rise in the DT signal at the QD excited and ground state energies.

The rise time of the QD n=2 signal (Fig. 4(a)) is also due to electron capture into the QDs, which is governed by Auger carrier-carrier scattering processes.[31, 32] According to refs. [31] and [33], efficient Auger relaxation will occur for photoexcited carrier densities greater than 10^{11} cm^{-2}. Both electron-electron scattering and electron-hole scattering are expected to influence the observed dynamics. However, for the carrier densities used in these measurements (~1.8×10^{11} cm^{-2}), electron-electron scattering rates are calculated to be approximately two orders of magnitude larger than electron-hole scattering rates,[33, 34] allowing us to identify this as the main channel for QD electron capture. In this scenario, two electrons in the QW states will scatter via an Auger process, with one electron relaxing into the QD n=2 state and the other electron ejected to higher QW states. Electrons can also be directly captured to the QD n=1 state through Auger scattering,[35] although the large energy separation between the QD n=1 state and the lowest QW state (Fig. 1(d)) makes it much less probable than capture to the QD n=2 state.[33]

We can eliminate other possible avenues for QD carrier capture through examining the energy level schematic of Fig. 1(d) while also considering the temperature and fluence dependence of the QD n=2 rise time. The existence of a finite

continuum of states, typically extending from the bulk band edge to below the QD n=2 state, has been suggested as a mechanism for fast carrier relaxation in certain quantum dot structures.[19, 30, 36, 37] These continuum states are believed due to intrinsic crossed transitions between delocalized wetting layer/barrier states and bound QD states (e.g., from a GaAs valence band state to the QD n=1 conduction band state).[38] Therefore, when two particles are located in a QD excited state with energy higher than a crossed transition, the bound state will autoionize, with the final state composed of one particle in a lower energy bound state and another particle ejected into the continuum.[33, 38]

In our DWELL structure, the presence of the QW lowers the QD energy levels relative to the bulk band edge.[3, 25] Therefore, the crossed bound-continuum transitions have higher energies than the QD n=2 transition, unlike in many conventional self-assembled QD heterostructures.[38] The lowest energy DWELL bound-continuum transition is between the GaAs valence band and QD n=1 conduction band state, calculated from Fig. 1(d) to be at 970 nm (1.28 eV). This crossed transition has a higher energy than the 1.18 eV QD n=2 transition, making autoionization of the n=2 state unlikely. Relaxation through a finite continuum of states thus cannot explain the observed rapid carrier capture into the QDs in our DWELL heterostructure. However, we cannot rule out contributions from a crossed transition between the GaAs continuum valence band states and the QD n=1 conduction band state to the 977 nm peak in the DT spectrum at 30 K.[37]

We can eliminate carrier-phonon scattering as a possible mechanism for the fast rise at the QD n=2 state by noting that the separation between the lowest QW state and n=2 QD state is ~88 meV, making electron capture into the QD through single phonon emission impossible and capture through multiphonon emission very unlikely for energy separations that are not an exact multiple of the LO phonon energy (ω_{LO}=32 meV for InAs).[39, 40] Further support comes from noting that the rise times measured at all wavelengths do not depend significantly on temperature (section 4), which contradicts a phonon-assisted process.[41] This also backs the minimal role of relaxation through a finite continuum of states in QD carrier capture, as this process is also expected to be temperature-dependent.[36] Finally, our fluence-dependent data (discussed in section 5 below) is also consistent with an Auger scattering process, as it reveals a rise time that decreases with pump fluence at the QD excited state.[32, 36] We can therefore isolate electron-electron scattering as the mechanism for carrier capture into the QD n=2 state.

Electron relaxation from the QD n=2 state to the n=1 conduction band states, manifested in the rise time of the QD n=1 DT signal (Fig. 4(a)), occurs through electron-hole scattering. The ~38 meV separation between the QD n=2 and n=1 conduction band states suggests that carrier-phonon scattering is not significant at this temperature. Auger electron-electron scattering does not conserve energy for this process, due to the lack of nearby continuum states for an electron to scatter into (Fig. 1(d)). However, the holes can easily scatter with phonons to higher energies due to the dense spacing of levels in the valence band, conserving energy and allowing the electrons to relax from the QD n=2 to n=1 states.[26, 39, 40, 42] This relaxation mechanism is expected to be quite efficient for the photoexcited carrier density used in these experiments. It is worth noting that intraband-pump, interband-probe experiments on self-assembled QDs that were doped with 4 electrons/dot clearly showed a sequential relaxation between QD levels in the absence of any holes.[43] Our experiments, conducted with approximately the same number of electron-hole pairs per dot, reveal rapid filling of the QD ground state through electron-hole scattering, further demonstrating the impact of this process on energy relaxation in quantum dots.

Figure 4(b) depicts the temporally resolved dynamics at long time delays. The long relaxation at the QD n=1 ground state is due to electron-hole recombination, occurring on a time scale of ~1 ns as determined from curve fits. The aforementioned long-lived DT signal at the QD n=2 excited state is due to state filling, as electron relaxation from the n=2 state will be inhibited once two electrons have filled the n=1 ground state.[6, 13] It is worth mentioning that although the conduction band spacing between the QD n=2 and n=1 states (~38 meV) is larger than the InAs LO phonon energy (~32 meV), electron-hole scattering prevents the observation of a phonon bottleneck.[29] The DT signal at the lowest QW state is also relatively long-lived (~185 ps), which is unexpected as the QD levels can accommodate all 4 photoexcited electron-hole pairs. This may be due to electron-hole scattering, which can scatter electrons into the lowest QW state from the QD n=2 state. However, further investigation is required to isolate the mechanism for the long-lived signal at the lowest QW state. In general, the relatively high photoexcited carrier density in these experiments makes it difficult to extract unambiguous lifetimes for bound-to-bound transitions (i.e., the QD n=2 to n=1 transition).

4. TEMPERATURE-DEPENDENT CARRIER DYNAMICS AT LOW CARRIER DENSITIES

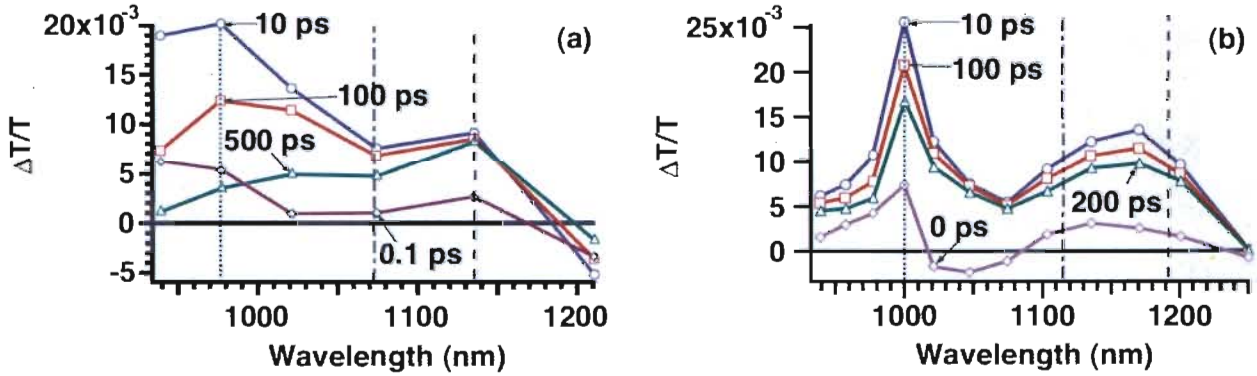

Figure 5. Differential transmission spectrum taken at N=4 ehp/dot at (a) 150 K and (b) 295 K. The approximate positions of the QW n=1, QD n=2, and QD n=1 states are indicated by the dotted, dot-dashed, and dashed lines, respectively. Part (b) is reprinted from ref. [23] with permission.

We now examine the temperature dependence of DWELL carrier dynamics at N=4 ehp/dot. Differential transmission spectra taken at 150 K and 295 K are depicted in Figure 5 for different time delays. The DT spectrum measured at 150 K was very similar to the 30 K DT spectrum (Fig. 3), indicating that the physical processes influencing carrier relaxation at 30 K should also apply at 150 K. In contrast, the most striking feature of the DT spectrum at 295 K is that its "camel back" shape stays approximately constant with increasing time delay, contrasting strongly with the 30 K DT spectrum (Fig. 3). This is a strong indication that thermal processes are redistributing the electron and hole populations among the confined QW and QD levels at high temperatures.[13, 41] In addition, the sharp peak at 1000 nm matches well with the QW n=1 transition observed in the PL spectra; its persistence with increasing time delay further indicates that carriers are thermally ejected from QD states into QW states at this temperature.

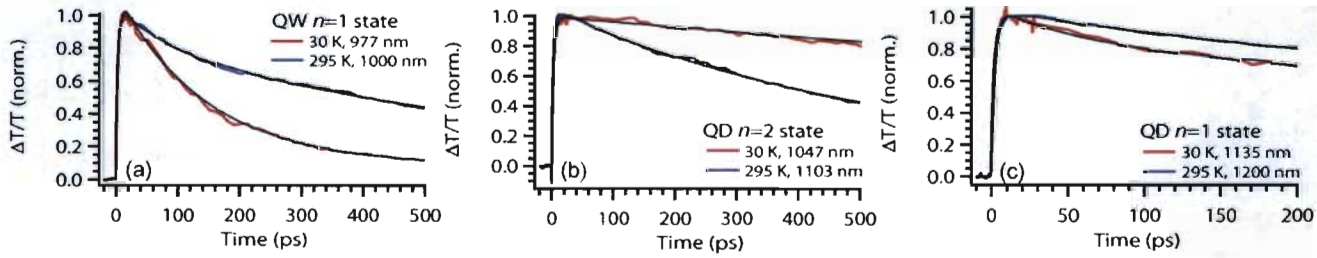

Figure 6. Normalized time-dependent DT signals at the (a) QW n=1, (b) QD n=2, and (c) QD n=1 states at 30 and 295 K. Reprinted from ref. [23] with permission.

Figure 6 compares individual time-resolved DT signals at the QW n=1, QD n=2, and QD n=1 transitions at 30 and 295 K, accounting for the red shift in these transitions as determined from the PL spectra (Fig. 1(b, c)). As described above, the lack of temperature dependence in the early time dynamics reveals that carrier capture into the QDs is due to Auger scattering, with minimal influence from phonon emission. Carrier relaxation dynamics are quite similar at 295 K for all probe wavelengths; curve fits show that the long time constant at 295 K exhibits relatively little variation (a factor of 2) over the measured wavelength range, unlike at 30 K where it varies by an order of magnitude. This indicates that carriers are both remitted and reabsorbed through thermal processes at room temperature, leading to a nearly energy-independent relaxation of electrons and holes at long times. The DT signal at the QW n=1 state persists for much longer times at 295 K than at 30 K, again due to thermal emission. As at 30 K, the QD n=2 DT signal at 295 K is long-lived (~1.1 ns), supporting the idea that state filling, not a phonon bottleneck, is responsible for this signal. In addition, the similarity between the QD n=1 DT signals indicates that recombination times do not change significantly with temperature in the DWELL heterostructure. Overall, the temperature dependence of the DT spectra, particularly the similarity between the 30 K and 150 K DT spectra, suggests the potential of DWELL-based devices for operating at

temperatures at least as high as 150 K; in fact, room temperature operation has recently been demonstrated in a DWELL-based photodetector.[44]

5. ULTRAFAST DENSITY-DEPENDENT CARRIER DYNAMICS AT LOW TEMPERATURES

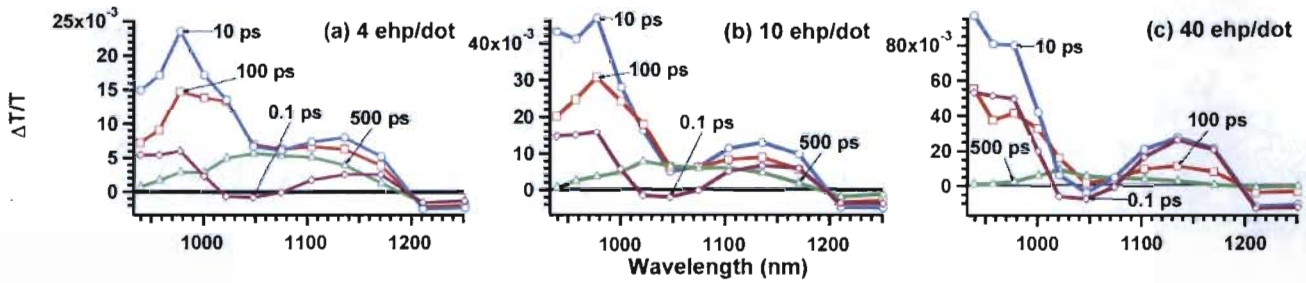

Figure 7. Differential transmission spectra for time delays of t=0.1, 10, 100, and 500 ps, taken at excitation densities of (a) 4 ehp/dot (1.8×10^{11} cm^{-2}), (b) 10 ehp/dot (4.5×10^{11} cm^{-2}), and (c) 40 ehp/dot (1.8×10^{12} cm^{-2}). The approximate positions of the QD ground and excited states are indicated by the dotted and dashed lines, respectively. Part (a) is identical to Fig. 3. Adapted from ref. [24] with permission.

Figure 7 shows the differential transmission spectra at several time delays and excitation densities. Here, we will focus on understanding the origins of the negative DT signal observed at the QD n=2 state (~1021-1074 nm) at early times and the long-lived negative DT signal observed for λ>1200 nm, which were briefly mentioned above in section 3. It is worth noting that similar long wavelength negative DT signals have been previously observed in InGaAs QDs embedded in bulk GaAs;[26] however, no anomalous signals were measured near the QD excited state in those studies. These negative signals typically signify a pump-induced absorption at the probe wavelength due to carrier density-dependent changes in the positions, amplitudes, and widths of the quantum confined optical transitions. In quantum dots, these effects arise at early times from Coulomb interactions between the pump-excited electron-hole pairs occupying a given quantized level and the electron-hole pair excited by the probe pulse;[12, 14] state filling typically causes these signals to turn positive at later times.

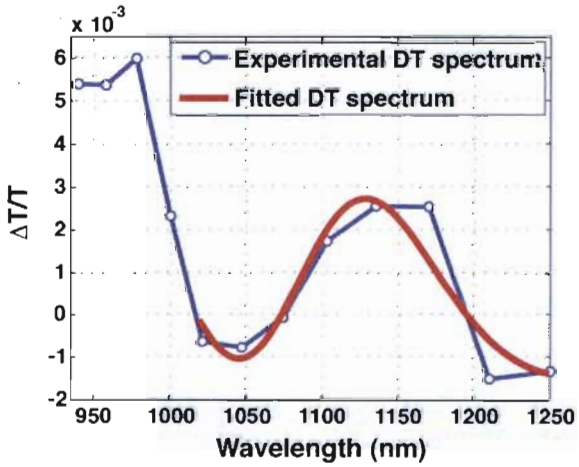

Figure 8. Experimental DT spectrum for N=4 ehp/dot and t=100 fs (blue circles) from Fig. 3(a) compared to the fitted curve generated by our model (red solid line) from 1021-1250 nm. Reprinted from ref. [24] with permission.

We have developed a simple model to more quantitatively understand the contribution of density-dependent changes in the optical transitions to the DT spectra. Generally, the DT spectrum for a given N, assuming that the photoinduced reflectivity change is negligible, is given by $\Delta T/T(t,\lambda) \approx -\Delta A/A(t,\lambda)$, with A the absorption. Then, $\Delta A(t,\lambda)=A_{PE}(t,\lambda)-A_0(t_0,\lambda)$, where $A_{PE}(t,\lambda)$ is the wavelength-dependent absorption at a time t>0 after photoexcitation. The absorption spectrum at a time t_0<0 before photoexcitation, $A_0(t_0,\lambda)$, can be modeled using Gaussian functions centered at the QD and QW states along with a continuum contribution from the QW, with spectral positions and widths obtained from our

PL experiments and amplitudes similar to those measured in refs. [37] and [45]. We can then vary the amplitudes, positions, and widths of the states comprising $A_{PL}(t,\lambda)$ to obtain $\Delta A(t,\lambda)$ and consequently $\Delta T/T(t,\lambda)$, thus allowing us to fit the experimentally observed DT spectrum for given values of t and N.

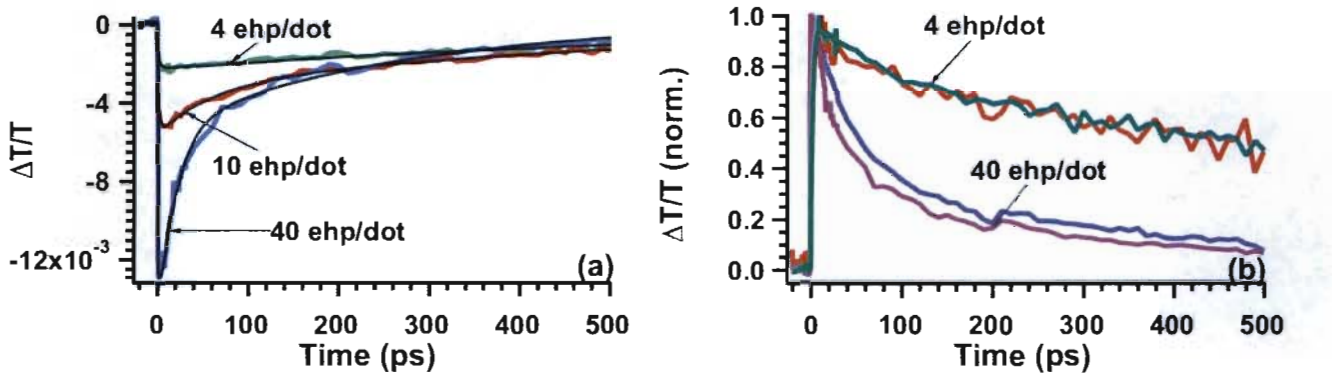

Figure 9. (a) Time-dependent DT signals for densities of N=4, 10, and 40 ehp/dot at 1250 nm. (b) Comparison between normalized DT signals at densities of 4 and 40 ehp/dot at 1135 nm (green, blue curves) and 1250 nm (red, purple curves). Adapted from ref. [24] with permission.

At N=4 ehp/dot, the negative features in the early time (t=100 fs) DT spectra can be consistently fit by varying the positions, amplitudes, and widths of the QD states, without including any contribution from the QW (Figure 8). This suggests that the early time DT spectra are dominated by carrier-induced red shifts of the QD levels, with typical magnitudes of a few tens of meV. Physically, as described in section 3, in this regime the pump pulse excites carriers above the GaAs band edge that rapidly relax into QW states through electron-phonon coupling and subsequently populate QD states through Auger carrier-carrier scattering.[23] For t<500 fs, the small (N<1) QD population causes the QD levels to redshift, resulting in negative DT signals at the shifted level positions.[12] However, within the first picosecond (ps) the QD population increases enough for the positive state filling-induced contribution to overwhelm the negative DT signal at the QD n=2 state (Fig. 7(a)).[12] In contrast, $\Delta T/T$ (1250 nm) remains negative for long times (Figure 9(a)) since there is no overlap with either QD transition and therefore no state filling-induced contribution. Our model indicates that this long wavelength signal can be directly linked to the QD ground state population and the resulting carrier-induced redshift of this state. This is further supported by Figure 9(b), which shows that at N=4 ehp/dot, the normalized $\Delta T/T$ (1250 nm) signal is nearly identical to the normalized $\Delta T/T$ (1135 nm) signal (which is proportional to the QD ground state population[23]). From this discussion we can conclude that at low carrier densities, the negative DT signals are likely due to QD level shifts, with little influence from the QW (although we cannot rule out such contributions, e.g. from direct transitions and shifts among QD states and QW/continuum states[35, 37]).

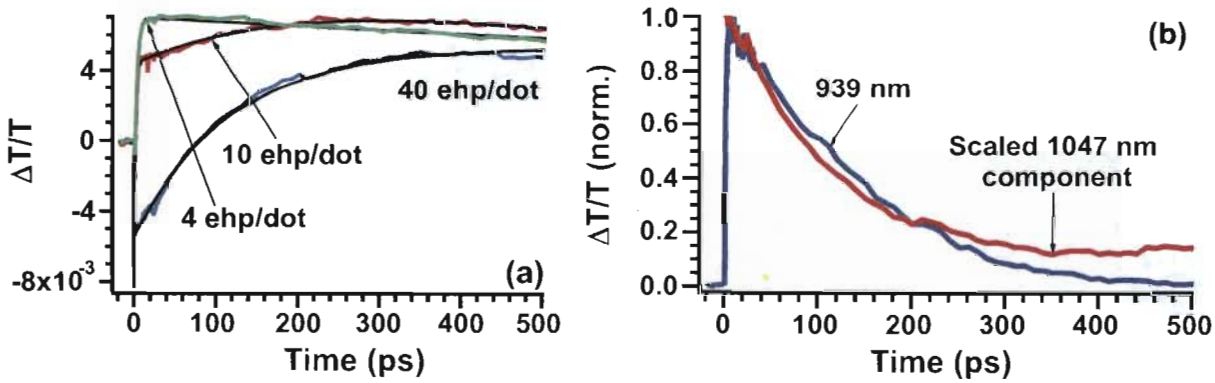

Figure 10. (a) Time-dependent DT signals for densities of N=4, 10, and 40 ehp/dot at 1047 nm. (b) Comparison between normalized DT signals at the QW n=1 state (939 nm) and the slowly recovering component of the 1047 nm DT signal (obtained from Fig. 10(a) by taking DT/T (t>2 ps), multiplying by -1 and scaling for comparison) at N=40 ehp/dot. Adapted from ref. [24] with permission.

As the carrier density increases, $\Delta T/T$ (1250 nm) remains negative throughout the measured temporal range (Fig. 9(a)) and continues to match $-\Delta T/T$ (1135 nm) (Fig. 9(b)). This indicates that this signal is due to population-induced shifts of the QD ground state at all measured densities. However, at 1047 nm an additional slowly recovering induced absorption component grows with carrier density, remaining negative for ~80 ps at N=40 ehp/dot (Figure 10(a)). The QD states are filled at N=6 ehp/dot,[35] after which extra carriers will populate the QW states. This implies that any density-dependent changes in the 1047 nm DT signal for N>6 ehp/dot can be linked to the QW population.

This is more quantitatively supported in Fig. 10(b), where we extract the slowly recovering component at 1047 nm and N=40 ehp/dot and scale it for comparison to the N=40 ehp/dot DT signal at the QW n=1 state (939 nm). Curve fits indicate that this signal relaxes with a time constant t=117 ps, while t=142 ps for the 939 nm signal. The close correspondence between these two signals for t<200 ps strongly suggests that the density-dependent induced absorption observed at the QD n=2 state is connected to the QW population. Physically, the 1047 nm signal is dominated by the QW population-induced absorption from t~2-200 ps; as t increases the QW population decays and its influence on the 1047 nm DT signal correspondingly diminishes, until at long times (t>300 ps) the 1047 nm signal reflects the intrinsic QD population dynamics, as at lower densities (Fig. 10(a)). Further studies will be required to unravel the mechanisms underlying the coupling between the QW population and light absorption at 1047 nm. Some compelling possibilities include carrier-induced shifts of the QW continuum band edge,[15] QD level shifts induced by the 2D carrier density, or excitation-induced dephasing.[16]

It is worth re-emphasizing that this link between the QW population and light absorption near the QD excited state has not been previously discovered in conventional QDs that are embedded in bulk materials, even when a negative long wavelength DT signal similar to that seen here was observed.[26] This suggests that the intentional introduction of a QW layer into a QD nanostructure (as compared to the wetting layer that is often present in conventional InGaAs/GaAs nanostructures) is critical for observing this phenomenon. More importantly, although the observed coupling between the QW population and light absorption at the QD n=2 state will likely affect DWELL-based lasers, the degree of control over nanostructure properties offered by the DWELL design should allow us to harness this phenomenon for many potential nanophotonic applications, such as dynamically tunable lasers and excitation-dependent optical switches.

6. CONCLUSIONS

In conclusion, we have temporally resolved carrier relaxation in a quantum dots-in-a-well heterostructure using differential transmission spectroscopy. We find that electron-electron scattering governs electron capture into the QDs from the QWs, with electron relaxation from the QD n=2 to the QD n=1 state governed by electron-hole scattering at low temperatures. At higher temperatures, thermal emission plays a significant role in the measured dynamics, distributing the electron and hole populations among many adjacent levels. Finally, our density-dependent studies reveal the influence of Coulomb interactions on the observed DT spectra across different time scales and excitation densities, highlighted by the observed influence of the QW population upon light absorption at the QD excited state. These experiments are a first step towards understanding carrier capture and relaxation across multiple spatial dimensions, with implications for DWELL-based lasers and photodetectors. Future work will focus on measuring ultrafast dynamics at lower carrier densities, directly pumping the excited state to examine gain dynamics, and performing ultrafast pump-probe experiments at longer mid-infrared to terahertz wavelengths.

ACKNOWLEDGMENTS

We would like to thank A. Gin, R. Averitt, S. Trugman, G. Jolley, T. Vandervelde, J. Shao, N. Weisse-Bernstein, P. Rotella, and A. Stintz for experimental assistance and helpful discussions. This work was performed at the Center for Integrated Nanotechnologies, a U.S. Department of Energy, Office of Basic Energy Sciences user facility. Los Alamos National Laboratory, an affirmative action equal opportunity employer, is operated by Los Alamos National Security, LLC, for the National Nuclear Security Administration of the U. S. Department of Energy under contract DE-AC52-06NA25396. We also acknowledge support from AFRL Contract FA9453-07-C-0171.

REFERENCES

[1] P. Bhattacharya, S. Ghosh, and A. D. Stiff-Roberts,"Quantum dot opto-electronic devices," Annu. Rev. Mater. Res. **34**, 1 (2004).

[2] C. B. Murray, D. J. Norris, and M. G. Bawendi,"Synthesis and characterization of nearly monodisperse CdE (E=S, Se, Te) semiconductor nanocrystallites," J. Am. Chem. Soc. **115**, 8706 (1993).

[3] S. Raghavan, P. Rotella, A. Stintz, B. Fuchs, S. Krishna, C. Morath, D. A. Cardimona, and S. W. Kennerly,"High-responsivity, normal-incidence long-wave infrared (λ~7.2 μm) InAs/$In_{0.15}Ga_{0.85}As$ dots-in-a-well detector," Appl. Phys. Lett. **81**, 1369 (2002).

[4] G. T. Liu, A. Stintz, H. Li, T. C. Newell, A. L. Gray, P. M. Varangis, K. J. Malloy, and L. F. Lester,"The influence of quantum-well composition on the performance of quantum dot lasers using InAs/InGaAs dots-in-a-well (DWELL) structures," IEEE J. Quant. Elect. **36**, 1272 (2000).

[5] J. Shah, *Ultrafast spectroscopy of semiconductors and semiconductor nanostructures* (Springer, New York, 1999).

[6] V. I. Klimov,"Spectral and dynamical properties of multiexcitons in semiconductor nanocrystals," Annu. Rev. Phys. Chem. **58**, 635 (2007).

[7] S. Krishna,"Quantum dots-in-a-well infrared photodetectors," J. Phys. D: Appl. Phys. **38**, 2142 (2005).

[8] L. F. Lester, A. Stintz, H. Li, T. C. Newell, E. A. Pease, B. A. Fuchs, and K. J. Malloy,"Optical characteristics of 1.24-um InAs quantum-dot laser diodes," IEEE Phot. Tech. Lett. **11**, 991 (1999).

[9] H. Su and L. F. Lester,"Dynamic properties of quantum dot distributed feedback lasers: high speed, linewidth, and chirp," J. Phys. D: Appl. Phys. **38**, 2112 (2005).

[10] J. Gomis-Bresco, et al.,"Impact of Coulomb scattering on the ultrafast gain recovery in InGaAs quantum dots," Phys. Rev. Lett. **101**, 256803 (2008).

[11] W. W. Chow and S. W. Koch,"Theory of semiconductor quantum-dot laser dynamics," IEEE J. Quant. Elect. **41**, 495 (2005).

[12] V. I. Klimov,"Optical nonlinearities and ultrafast carrier dynamics in semiconductor nanocrystals," J. Phys. Chem. B **104**, 6112 (2000).

[13] T. B. Norris, K. Kim, J. Urayama, Z. K. Wu, J. Singh, and P. Bhattacharya,"Density and temperature dependence of carrier dynamics in self-organized InGaAs quantum dots," J. Phys. D: Appl. Phys. **38**, 2077 (2005).

[14] P. Borri, S. Schneider, W. Langbein, and D. Bimberg,"Ultrafast carrier dynamics in InGaAs quantum dot materials and devices," J. Opt. A: Pure Appl. Opt. **8**, S33 (2006).

[15] H. C. Schneider, W. W. Chow, and S. W. Koch,"Many-body effects in the gain spectra of highly excited quantum-dot lasers," Phys. Rev. B **64**, 115315 (2001).

[16] H. C. Schneider, W. W. Chow, and S. W. Koch,"Excitation-induced dephasing in semiconductor quantum dots," Phys. Rev. B **70**, 235308 (2004).

[17] A. Fiore, P. Borri, W. Langbein, J. M. Hvam, U. Oesterle, R. Houdre, R. P. Stanley, and M. Ilegems,"Time-resolved optical characterization of InAs/InGaAs quantum dots emitting at 1.3 um," Appl. Phys. Lett. **76**, 3430 (2000).

[18] A. I. Tartakovskii, R. S. Kolodka, H. Y. Liu, M. A. Migliorato, M. Hopkinson, M. N. Makhonin, D. J. Mowbray, and M. S. Skolnick,"Exciton fine structure splitting in dot-in-a-well structures," Appl. Phys. Lett. **88**, 131115 (2006).

[19] G. Raino, G. Visimberga, A. Salhi, M. De Vittorio, A. Passaseo, R. Cingolani, and M. De Giorgi,"Simultaneous filling of InAs quantum dot states from the GaAs barrier under nonresonant excitation," Appl. Phys. Lett. **90**, 111907 (2007).

[20] I. O'Driscoll, T. Piwonski, C.-F. Schleussner, J. Houlihan, G. Huyet, and R. J. Manning,"Electron and hole dynamics of InAs/GaAs quantum dot semiconductor optical amplifiers," Appl. Phys. Lett. **91**, 071111 (2007).

[21] T. Piwonski, J. Pulka, G. Madden, G. Huyet, J. Houlihan, E. A. Viktorov, T. Erneux, and P. Mandel,"Intradot dynamics of InAs quantum dot based electroabsorbers," Appl. Phys. Lett. **94**, 123504 (2009).

[22] P. Aivaliotis, S. Menzel, E. A. Zibik, J. W. Cockburn, L. R. Wilson, and M. Hopkinson,"Energy level structure and electron relaxation times in InAs/$In_xGa_{1-x}As$ quantum dot-in-a-well structures," Appl. Phys. Lett. **91**, 253502 (2007).

[23] R. P. Prasankumar, R. S. Attaluri, R. D. Averitt, J. Urayama, N. Weisse-Bernstein, P. Rotella, A. Stintz, S. Krishna, and A. J. Taylor,"Ultrafast carrier dynamics in an InAs/InGaAs quantum dots-in-a-well heterostructure," Opt. Express **16**, 1165 (2008).

[24] R. P. Prasankumar, W. W. Chow, J. Urayama, R. S. Attaluri, R. Shenoi, S. Krishna, and A. J. Taylor,"Density-dependent carrier dynamics in a quantum dots-in-a-well heterostructure," Appl. Phys. Lett. **96**, 031110 (2010).

[25] S. Krishna, S. Raghavan, G. von Winckel, P. Rotella, A. Stintz, C. P. Morath, D. Le, and S. W. Kennerly,"Two color InAs/InGaAs dots-in-a-well detector with background-limited performance at 91 K," Appl. Phys. Lett. **82**, 2574 (2003).

[26] T. S. Sosnowski, T. B. Norris, H. Jiang, J. Singh, K. Kamath, and P. Bhattacharya,"Rapid carrier relaxation in $In_{0.4}Ga_{0.6}As$/GaAs quantum dots characterized by differential transmission spectroscopy," Phys. Rev. B **57**, R9423 (1998).

[27] R. P. Prasankumar, P. C. Upadhya, and A. J. Taylor,"Ultrafast carrier dynamics in semiconductor nanowires," Physica Status Solidi(b) **246**, 1973 (2009).

[28] F. Quochi, M. Dinu, L. N. Pfeiffer, K. W. West, C. Kerbage, R. S. Windeler, and B. J. Eggleton,"Coulomb and carrier-activation dynamics of resonantly excited InAs/GaAs quantum dots in two-color pump-probe experiments," Phys. Rev. B **67**, 235323 (2003).

[29] J. Urayama, T. B. Norris, J. Singh, and P. Bhattacharya,"Observation of phonon bottleneck in quantum dot electronic relaxation," Phys. Rev. Lett. **86**, 4930 (2001).

[30] Y. Toda, O. Moriwaki, M. Nishioka, and Y. Arakawa,"Efficient carrier relaxation mechanism in InGaAs/GaAs self-assembled quantum dots based on the existence of continuum states," Phys. Rev. Lett. **82**, 4114 (1999).

[31] U. Bockelmann and T. Egeler,"Electron relaxation in quantum dots by means of Auger processes," Phys. Rev. B **46**, 15574 (1992).

[32] B. Ohnesorge, M. Albrecht, J. Oshinowo, A. Forchel, and Y. Arakawa,"Rapid carrier relaxation in self-assembled InxGa1-xAs/GaAs quantum dots," Phys. Rev. B **54**, 11532 (1996).

[33] R. Ferreira and G. Bastard,"Unbound states in quantum heterostructures," Nanoscale Res. Lett. **1**, 120 (2006).

[34] A. V. Uskov, J. McInerney, F. Adler, H. Schweizer, and M. H. Pilkuhn,"Auger carrier capture kinetics in self-assembled quantum dot structures," Appl. Phys. Lett. **72**, 58 (1998).

[35] J. Urayama, T. B. Norris, H. Jiang, J. Singh, and P. Bhattacharya,"Differential transmission measurement of phonon bottleneck in self-assembled quantum dot intersubband relaxation," Physica B **316-317**, 74 (2002).

[36] E. W. Bogaart, J. E. M. Haverkort, T. Mano, T. van Lippen, R. Notzel, and J. H. Wolter,"Role of the continuum background for carrier relaxation in InAs quantum dots," Phys. Rev. B **72**, 195301 (2005).

[37] G. Visimberga, et al.,"Evidence of "crossed" transitions in dots-in-a-well structures through waveguide absorption measurements," Appl. Phys. Lett. **93**, 151112 (2008).

[38] A. Vasanelli, R. Ferreira, and G. Bastard,"Continuous absorption background and decoherence in quantum dots," Phys. Rev. Lett. **89**, 216804 (2002).

[39] R. Ferreira and G. Bastard,"Phonon-assisted capture and intradot Auger relaxation in quantum dots," Appl. Phys. Lett. **74**, 2818 (1999).

[40] H. Jiang and J. Singh,"Radiative and non-radiative inter-subband transition in self-assembled quantum dots," Physica E **2**, 720 (1998).

[41] J. Urayama, T. B. Norris, H. Jiang, J. Singh, and P. Bhattacharya,"Temperature-dependent carrier dynamics in self-assembled InGaAs quantum dots," Appl. Phys. Lett. **80**, 2162 (2002).

[42] J. Siegert, S. Marcinkevicius, and Q. X. Zhao,"Carrier dynamics in modulation-doped InAs/GaAs quantum dots," Phys. Rev. B **72**, 085316 (2005).

[43] Z.-K. Wu, H. Choi, X. Su, S. Chakrabarti, P. Bhattacharya, and T. B. Norris,"Ultrafast electronic dynamics in unipolar n-doped InGaAs-GaAs self-assembled quantum dots," IEEE J. Quant. Elect. **43**, 486 (2007).

[44] H. Lim, S. Tsao, W. Zhang, and M. Razeghi,"High-performance InAs quantum-dot infrared photodetectors grown on InP substrate operating at room temperature," Appl. Phys. Lett. **90**, 131112 (2007).

[45] L. E. Vorobjev, et al.,"Interband light absorption and Pauli blocking in InAs/GaAs quantum dots covered by InGaAs quantum wells," Semicond. Sci. Technol. **22**, 814 (2007).